

Identification of *Osr2* Transcriptional Target Genes in Palate Development

Journal of Dental Research
2017, Vol. 96(12) 1451–1458
© International & American Associations
for Dental Research 2017
Reprints and permissions:
sagepub.com/journalsPermissions.nav
DOI: 10.1177/0022034517719749
journals.sagepub.com/home/jdr

X. Fu¹, J. Xu¹, P. Chaturvedi¹, H. Liu¹, R. Jiang^{1,2}, and Y. Lan^{1,2}

Abstract

Previous studies have identified the odd-skipped related 2 (*Osr2*) transcription factor as a key intrinsic regulator of palatal shelf growth and morphogenesis. However, little is known about the molecular program acting downstream of *Osr2* in the regulation of palatogenesis. In this study, we isolated palatal mesenchyme cells from embryonic day 12.5 (E12.5) and E13.5 *Osr2*^{RFP/+} and *Osr2*^{RFP/-} mutant mouse embryos and performed whole transcriptome RNA sequencing analyses. Differential expression analysis of the RNA sequencing datasets revealed that expression of 70 genes was upregulated and expression of 61 genes was downregulated by >1.5-fold at both E12.5 and E13.5 in the *Osr2*^{RFP/-} palatal mesenchyme cells, in comparison with *Osr2*^{RFP/+} littermates. Gene ontology analysis revealed enrichment of signaling molecules and transcription factors crucial for skeletal development and osteoblast differentiation among those significantly upregulated in the *Osr2* mutant palatal mesenchyme. Using quantitative real-time polymerase chain reaction (RT-PCR) and in situ hybridization assays, we validated that the *Osr2*^{-/-} embryos exhibit significantly increased and expanded expression of many osteogenic pathway genes, including *Bmp3*, *Bmp5*, *Bmp7*, *Mef2c*, *Sox6*, and *Sp7* in the developing palatal mesenchyme. Furthermore, we demonstrate that expression of *Sema3a*, *Sema3d*, and *Sema3e*, is ectopically activated in the developing palatal mesenchyme in *Osr2*^{-/-} embryos. Through chromatin immunoprecipitation, followed by RT-PCR analysis, we demonstrate that endogenous *Osr2* protein binds to the promoter regions of the *Sema3a* and *Sema3d* genes in the embryonic palatal mesenchyme. Moreover, *Osr2* expression repressed the transcription from the *Sema3a* and *Sema3d* promoters in cotransfected cells. Since the *Sema3* subfamily of signaling molecules plays diverse roles in the regulation of cell proliferation, migration, and differentiation, these data reveal a novel role for *Osr2* in regulation of palatal morphogenesis through preventing aberrant activation of *Sema3* signaling. Together, these data indicate that *Osr2* controls multiple molecular pathways, including BMP and *Sema3* signaling, in palate development.

Keywords: cleft palate, craniofacial biology, gene expression, morphogenesis, osteogenesis, signal transduction

Introduction

Cleft palate affects about 1 in 1,000 live births worldwide and is one of the most common structural birth defects in humans (Dixon et al. 2011). Although genetic and genome-wide association studies of human populations, as well as genetic and developmental biology studies in animal models, have identified a large number of genes associated with cleft palate formation, the molecular mechanisms regulating palate development are still not well understood (Dixon et al. 2011; Bush and Jiang 2012; Funato et al. 2015; Lan et al. 2015). In particular, whereas tissue-specific genetic studies have shown that many signaling pathways and transcription factors play crucial roles in palatal shelf growth and patterning (Bush and Jiang 2012; Lane and Kaartinen 2014; Lan et al. 2015), little is known about the transcriptional regulatory networks functioning in the signaling pathways and the cellular processes during palatogenesis.

Through developmental gene expression screening and targeted mutagenesis studies in mice, we previously identified the odd-skipped related 2 (*Osr2*) transcription factor as a key regulator of palatal shelf growth and patterning (Lan et al. 2001; Lan et al. 2004). During mouse embryogenesis, *Osr2* mRNA expression is specifically activated in the palatal mesenchyme at the onset of palatal shelf outgrowth (Lan et al. 2001; Lan et al.

2004). As palatal shelves grow vertically along the sides of the developing tongue, expression of *Osr2* mRNAs exhibits a lateral-to-medial gradient in the palatal mesenchyme (Lan et al. 2004). Mice lacking *Osr2* exhibit cleft palate due to impaired palatal mesenchyme proliferation and delay in palatal shelf elevation (Lan et al. 2004). Although no pathogenic mutation in *OSR2* has been reported in cleft palate patients, the human *OSR2* gene is located at chromosome 8q23, a region strongly associated with nonsyndromic orofacial clefting (Prescott et al.

¹Division of Developmental Biology, Cincinnati Children's Hospital Medical Center, Cincinnati, OH, USA

²Division of Plastic Surgery, Cincinnati Children's Hospital Medical Center, Cincinnati, OH, USA

A supplemental appendix to this article is available online.

Corresponding Authors:

R. Jiang, Division of Developmental Biology, Cincinnati Children's Hospital Medical Center, MLC 7007, 3333 Burnet Avenue, Cincinnati, OH 45229, USA.

Email: Rulang.Jiang@cchmc.org

Y. Lan, Division of Plastic Surgery, Cincinnati Children's Hospital Medical Center, MLC 7007, 3333 Burnet Avenue, Cincinnati, OH 45229, USA.

Email: Yu.Lan@cchmc.org

2000). Moreover, mice with palatal mesenchyme-specific inactivation of *Smoothed*, which encodes an obligatory transducer of hedgehog signaling, exhibit loss of *Osr2* expression in the palatal mesenchyme and significant reduction in palatal mesenchyme proliferation, suggesting that *Osr2* acts downstream of hedgehog signaling to control palatal shelf growth (Lan and Jiang 2009). Furthermore, mice lacking the Pax9 transcription factor exhibit cleft palate due to defects in palatal mesenchyme proliferation and failure of palatal shelf elevation (Peters et al. 1998; Zhou et al. 2013). Pax9 function is required for maintenance of *Osr2* expression in the palatal mesenchyme and for restoration of *Osr2* expression in the palatal mesenchyme partly rescued palatogenesis in the absence of Pax9 function (Zhou et al. 2013), indicating that *Osr2* is an important mediator of Pax9 regulation of palate development. Recently, Almaidhan et al. (2014) showed that mice with neural crest-specific deletion of *Ldb1*—which encodes LIM domain-binding protein-1 that can interact with multiple LIM domain-containing transcription factors—exhibit defects in palatal shelf growth and elevation, accompanied by aberrant upregulation of *Osr2* expression in the palatal mesenchyme. Together, these studies indicate that multiple molecular pathways converge on the regulation of *Osr2* expression during palate development. However, little is known about the target genes that mediate *Osr2* function in palate development.

In this study, we used fluorescence-activated cell sorting (FACS) to isolate developing palatal mesenchyme from *Osr2* heterozygous and homozygous mutant mouse embryos and performed RNA sequencing (RNA-seq) analyses. Gene ontology analysis of *Osr2*-dependent gene expression profiles identified a major role for *Osr2* in suppressing osteogenic differentiation of the palatal mesenchyme. Moreover, we found that *Osr2* directly represses expression of several members of the class 3 semaphorins in the developing palatal mesenchyme. These results provide novel insight into the molecular mechanisms involving *Osr2* in palate development.

Materials and Methods

Mouse Strains

The *Osr2*^{+/-} (*Osr2*^{tm1Jian/+}), *Osr2*^{RFP/+}, *Osr2*^{Myc-Osr2AKi/+} mice have been described (Lan et al. 2004; Gao et al. 2009; Xu et al. 2016). *Osr2*^{+/-} and *Osr2*^{RFP/+} mice were maintained by crossing to C57BL/6J inbred mice. *Osr2*^{Myc-Osr2AKi/Myc-Osr2AKi} mice were maintained by intercrossing males and females in the stock background. For timed pregnancies, embryonic day 0.5 (E0.5) was defined as noon of the day that a vaginal plug was identified. This study was performed in accordance with the recommendations in the “Guide for the Care and Use of Laboratory Animals” by the National Institutes of Health. The animal use protocol was approved by the Institutional Animal Care and Use Committee of Cincinnati Children’s Hospital Medical Center (permit IACUC2016-0095). This study conformed with ARRIVE guidelines for preclinical animal studies.

Isolation of Palatal Mesenchyme with FACS

The palatal shelves of E12.5 and E13.5 *Osr2*^{RFP/+} and *Osr2*^{RFP/-} embryos were manually microdissected in cold sterile phosphate buffered saline (PBS) and digested with trypsin-EDTA (Invitrogen) at 37 °C for 4 min. After inactivation of trypsin with Dulbecco’s Modified Eagle’s Medium containing 10% fetal bovine serum (FBS), cells were dissociated by pipetting. The dissociated cells were suspended in PBS with 2% FBS and 10mM ethylenediaminetetraacetic acid (EDTA) and filtered through a 40- μ m nylon cell strainer (352340; BD Falcon). Red fluorescent protein (RFP)-positive cells were isolated with BD FACSAria II and immediately processed for total RNA isolation.

RNA-Seq and Data Analysis

Total RNAs were extracted from FACS-isolated palatal mesenchyme cells with the Qiagen RNeasy Micro Kit (74004; Qiagen). Sequencing libraries were generated with Illumina Nextera DNA Sample Prep Kit and sequenced with Illumina HiSeq 2000. Sequence reads were mapped to the reference mouse genome (mm9) with Bowtie. RNA-seq data were analyzed with Strand NGS software, with the FPKM value (fragments per kilobase exon per million mapped sequences) calculated for each RefSeq gene. For analyses of differential expression, the fold change cutoff was set at ≥ 1.5 -fold, and *P* values < 0.01 from the Audic-Claverie test were considered statistically significant, with Benjamini-Hochberg false discovery rate multiple testing correction (Brunskill and Potter 2012). Functional annotation analysis was carried out with online tools at <https://toppgene.cchmc.org>, as previously described (Chen et al. 2009). The RNA-seq data of this study have been deposited into the National Center for Biotechnology Information Gene Expression Omnibus database (accession GSE95638).

Quantitative RT-PCR

First-strand cDNAs were synthesized with the SuperScript First-Strand Synthesis System (11904-018; Invitrogen). Real-time polymerase chain reaction (RT-PCR) was performed with a Bio-Rad CFX96 Real-Time System with conditions recommended by the manufacturer. Each reaction was performed at least in triplicates. The quantity of each mRNA was first determined with a standard curve method and normalized to the level of *Hprt* mRNAs. The sequences of primers used for the quantitative RT-PCR (RT-qPCR) are listed in Appendix Table 1.

In Situ Hybridization

Whole mount and section in situ hybridization was performed as previously described (Zhang et al. 1999). At least 3 embryos of each genotype were hybridized to each probe, and only probes that detected consistent patterns of expression in all samples were considered valid results.

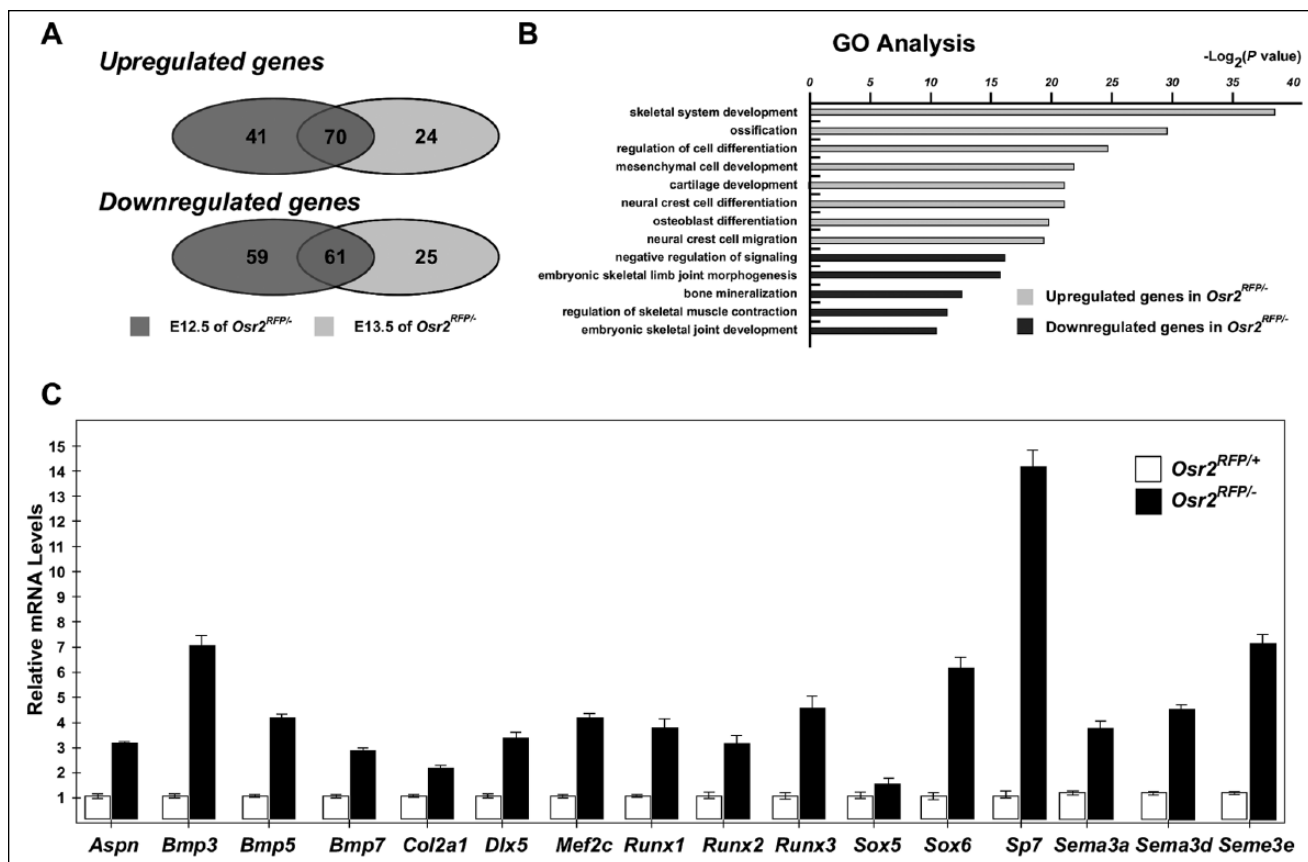


Figure 1. Effects of loss of *Osr2* function on palatal mesenchyme gene expression profiles revealed by RNA sequencing and RT-qPCR analyses. **(A)** Venn diagrams comparing genes whose expression was significantly up- or downregulated by at least 1.5-fold in the palatal mesenchyme in *Osr2*^{RFP/-} embryos as compared with *Osr2*^{RFP/+} embryos at embryonic day (E) 12.5 and E13.5. **(B)** Gene ontology (GO) analysis of the biological processes affected by the differentially expressed genes. **(C)** RT-qPCR validation of differential expression of select osteogenic pathway genes in E13.5 palatal mesenchyme cells in *Osr2*^{RFP/-} embryos in comparison with *Osr2*^{RFP/+} embryos. The level of expression of each gene in the *Osr2*^{RFP/+} samples is set to 1 for direct visualization of fold increase of expression in the *Osr2*^{RFP/-} samples. Error bars indicate standard error of the mean.

Chromatin Immunoprecipitation

The palatal shelves were microdissected from E13.5 *Osr2*^{Myc-Osr2AKI} homozygous embryos and crosslinked with 1.5% paraformaldehyde in crosslinking buffer (10mM NaCl, 0.1mM EDTA, 0.05mM egtazic acid [EGTA], 5mM hydroxyethyl piperazineethanesulfonic acid [HEPES], pH 8.0) at 37 °C for 45 min with constant shaking. Glycine was added to a final concentration of 125mM and incubated at 37 °C for 10 min to stop crosslinking. After washing with ice-cold PBS, cells were transferred into 1 mL of precooled lysis buffer (50mM HEPES, pH7.5, 0.14M NaCl, 1mM EDTA, 10% glycerol, 0.5% NP40, 0.25% Triton X-100) with protease inhibitors (SC-24948; Santa Cruz) and incubated at 4 °C for 10 min to release the cell nuclei. The sample was centrifuged at 3,600 rpm for 5 min. The cell nuclei pellet was suspended in buffer 2 (0.2M NaCl, 1mM EDTA, 0.5mM EGTA, 10mM Tris, pH 8.0), incubated at 4 °C for 5 min, and centrifuged at 3,600 rpm for 5 min. The pellet was then resuspended in buffer 3 (1mM EDTA, 0.5mM EGTA, 10mM Tris, pH 8.0), containing protease inhibitors, and sonicated 8 times at 30 s each, with 1-min intervals, on ice. Chromatin fragments were isolated by centrifuging at 8,000 rpm for 5 min. The chromatin solution was incubated with anti-c-MYC

monoclonal antibody (clone 4A6, 16-219; Millipore) for 2 h at 4 °C, followed by addition of protein G-conjugated Dynabeads and rotation overnight at 4 °C. The Dynabeads were washed 5 times with radio immunoprecipitation assay (RIPA) buffer (1% NP-40, 1% sodium deoxycholate, 1mM EDTA, 50mM HEPES pH 7.5, 0.5M LiCl). DNA was isolated from the immunoprecipitated complex, eluted in 150 μ L of elution buffer (50mM Tris pH 8.0, 10mM EDTA, 1% sodium dodecyl sulfate [SDS]), and amplified by real-time PCR with specific primers flanking candidate *Osr2* binding sites.

Cell Culture, Transfection, and Dual-Luciferase Reporter Assay

NIH/3T3 cells (CRL-1658; ATCC) were cultured in high-glucose Dulbecco's Modified Eagle's Medium containing 10% FBS, penicillin (100 IU/mL), and streptomycin (100 μ g/mL; Invitrogen) in 48-well plates and transfected with 1 μ L of Lipofectamine 3000 Reagent (Thermo Fisher Scientific) for each well, according to the manufacturer's instructions. Each luciferase reporter construct (0.4 μ g each: *pGL3-Sema3a-3k*, *pGL3-Sema3d-3k*, *pGL3-Sema3e-3k*) was transfected with or

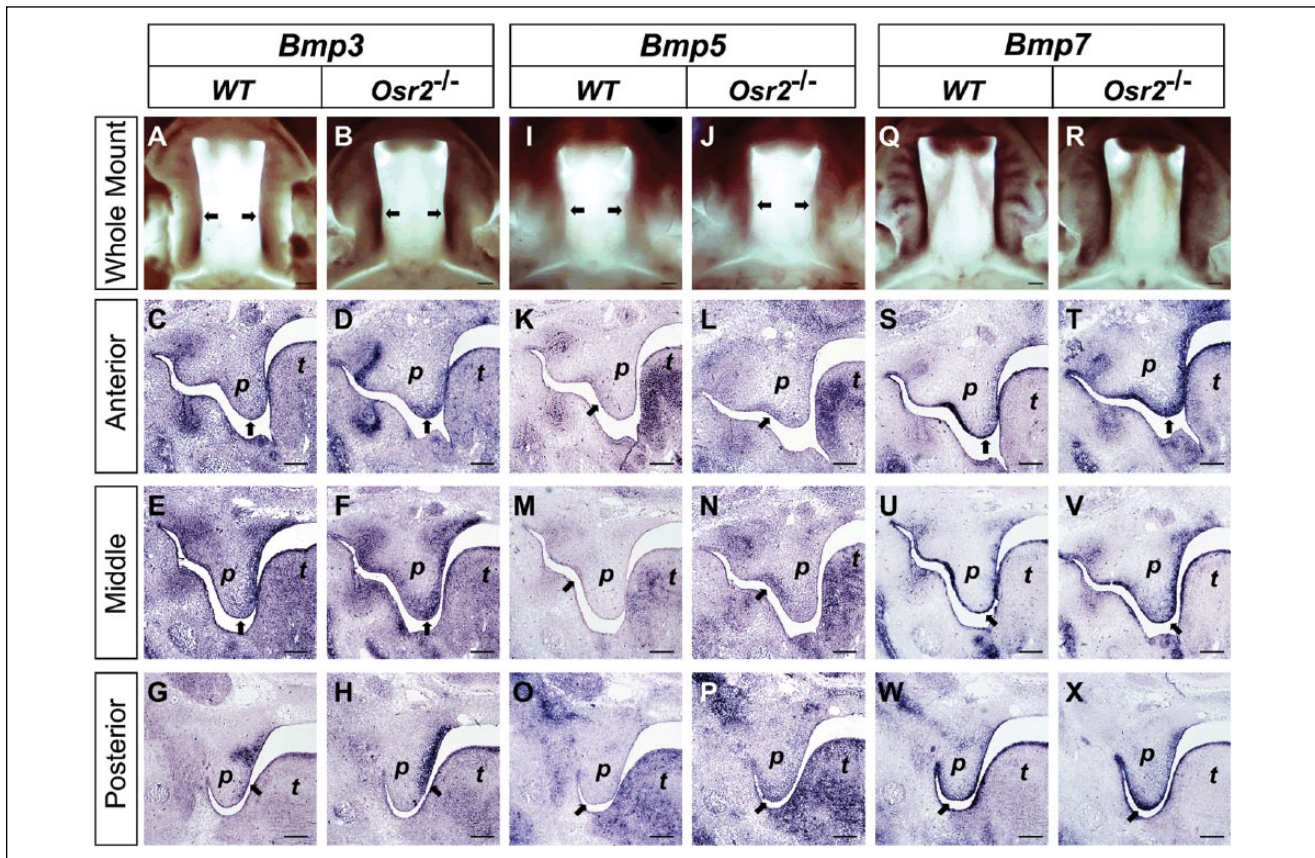


Figure 2. Comparison of patterns of expression of *Bmp3*, *Bmp5*, and *Bmp7* mRNAs in the palatal tissues in E13.5 *Osr2*^{-/-} mutant and wild-type embryos with whole mount and section in situ hybridization. Whole mount images (top row) show oral views of the palatal shelves, whereas the “anterior,” “middle,” and “posterior” rows show coronal sections from regions of the palatal shelves. (A–H) Expression patterns of *Bmp3* mRNAs. (I–P) Expression patterns of *Bmp5* mRNAs. (Q–X) Expression patterns of *Bmp7* mRNAs. Arrows point to regions of differential expression. p, palatal shelf; t, tongue. Scale bars, 100 μm.

without 0.2 μg of *pCMV-3XFLAG-Osr2* expression vector (Zhou et al. 2011) and 10 ng of pRL-TK plasmid (internal control). Luciferase activities of firefly and Renilla were measured 48 h after transfection with the dual-luciferase reporter assay system (Promega). Data were collected from at least 3 independent replicate assays.

Results

Effects of Loss of *Osr2* Function on Palatal Mesenchyme Gene Expression

To gain a better understanding of the molecular mechanisms mediating *Osr2* function in palate development, we performed RNA-seq analysis of transcriptome expression profiles of the developing palatal mesenchyme in *Osr2*^{-/-} and control littermates. As we have shown previously, mice carrying the *Osr2*^{RFP} knockin/knockout allele express the RFP reporter in all *Osr2*-expressing cells, including embryonic palatal shelf mesenchyme (Xu et al. 2016). We crossed *Osr2*^{RFP/+} male mice with *Osr2*^{+/-} female mice—which carry a lacZ reporter cassette replacing the coding region of the *Osr2* gene (Lan et al.

2004)—microdissected palatal shelves from *Osr2*^{RFP/+} and *Osr2*^{RFP/-} embryos at E12.5 and E13.5, respectively, and processed for FACS isolation of RFP-positive cells from each embryo. RNA-seq analyses were carried for 1 pair of E12.5 and 2 pairs of E13.5 embryos. Differential expression analysis of the RNA-seq data sets identified 280 genes, in addition to *Osr2* itself, the expression of which was up- or downregulated by >1.5-fold in the *Osr2*^{RFP/-} palatal mesenchyme in comparison with the *Osr2*^{RFP/+} littermates, in which 70 genes were upregulated in E12.5 and E13.5 *Osr2*^{RFP/-} mutant palatal mesenchyme, whereas 61 genes were downregulated in E12.5 and E13.5 *Osr2*^{RFP/-} mutant palatal mesenchyme (Fig. 1A, Appendix Tables 2 and 3). We performed RT-qPCR analyses and verified that a number of signaling molecules and transcription factors important for the regulation of osteoblast differentiation or ossification—including *Bmp3*, *Bmp5*, *Bmp7*, *Dlx5*, *Mef2c*, *Runx2*, *Runx3*, *Sox6*, and *Sp7*—are upregulated by ≥2-fold in the palatal mesenchyme in *Osr2*^{RFP/-} mutant embryos in comparison with the *Osr2*^{RFP/+} control littermates (Fig. 1C). The significant downregulation of several genes in the palatal mesenchyme in *Osr2*^{RFP/-} mutant embryos, including *Igf1*, *Lhx8*, *Osr1*, and *Pcdh17*, was also validated by RT-qPCR analyses (Appendix Fig. 1).

Validation of *Osr2*-Dependent Gene Expression in the Developing Palatal Mesenchyme with *In Situ* Hybridization

To further validate effects of loss of *Osr2* function on palatal mesenchyme gene expression, we compared patterns of expression of select differentially expressed genes in the *Osr2*^{RFP/+} and *Osr2*^{RFP/-} embryonic palatal shelves by whole mount and section in situ hybridization. *Bmp3*, *Bmp5*, and *Bmp7* are expressed in distinct patterns along the anterior-posterior axis of the developing palatal shelves in wild-type embryos at E13.5, with *Bmp3* mRNAs expressed in the medial region of posterior palatal mesenchyme (Fig. 2A, C, E, G), *Bmp5* mRNAs preferentially expressed in the lateral side of anterior palatal mesenchyme (Fig. 2I, K, M, O), and *Bmp7* mRNAs strongly expressed throughout palatal epithelium (Fig. 2Q, S, U, W). In E13.5 *Osr2*^{-/-} mutant embryos, expression of *Bmp3* mRNAs is ectopically activated in the distal palatal mesenchyme in the anterior and middle regions of the palatal shelves (Fig. 2B, D, F), expression of *Bmp5* mRNAs is expanded to the middle and posterior regions of palatal mesenchyme (Fig. 2J, L, N, P), whereas expression of *Bmp7* mRNAs is increased in subepithelial regions of the palatal mesenchyme throughout the anterior-posterior axis (Fig. 2R, T, V, X). These results indicate that, although *Bmp3*, *Bmp5*, and *Bmp7* are differentially regulated during palate development, *Osr2* plays an important role in regulating expression of each in the developing palatal mesenchyme.

Comparative analysis of expression of genes associated with osteogenic differentiation, including *Aspn*, *Mef2c*, *Sox6*, and *Sp7*, confirmed that expression domain of each of these genes is expanded in the *Osr2*^{-/-} palatal mesenchyme in comparison with their wildtype littermates at E13.5 (Fig. 3). These data, with the previous finding that the *Osr2*^{-/-} embryos exhibit reduced palatal mesenchyme proliferation (Lan et al. 2004), suggest that *Osr2* regulates palate development in part through preventing premature osteogenic differentiation of palatal mesenchyme.

Osr2 Binds to the Promoter Regions and Negatively Regulates Expression of the *Sema3a* and *Sema3d* Genes in the Developing Palatal Mesenchyme

From differential expression analysis of the RNA-seq data sets, we found that 3 structurally homologous and physically linked

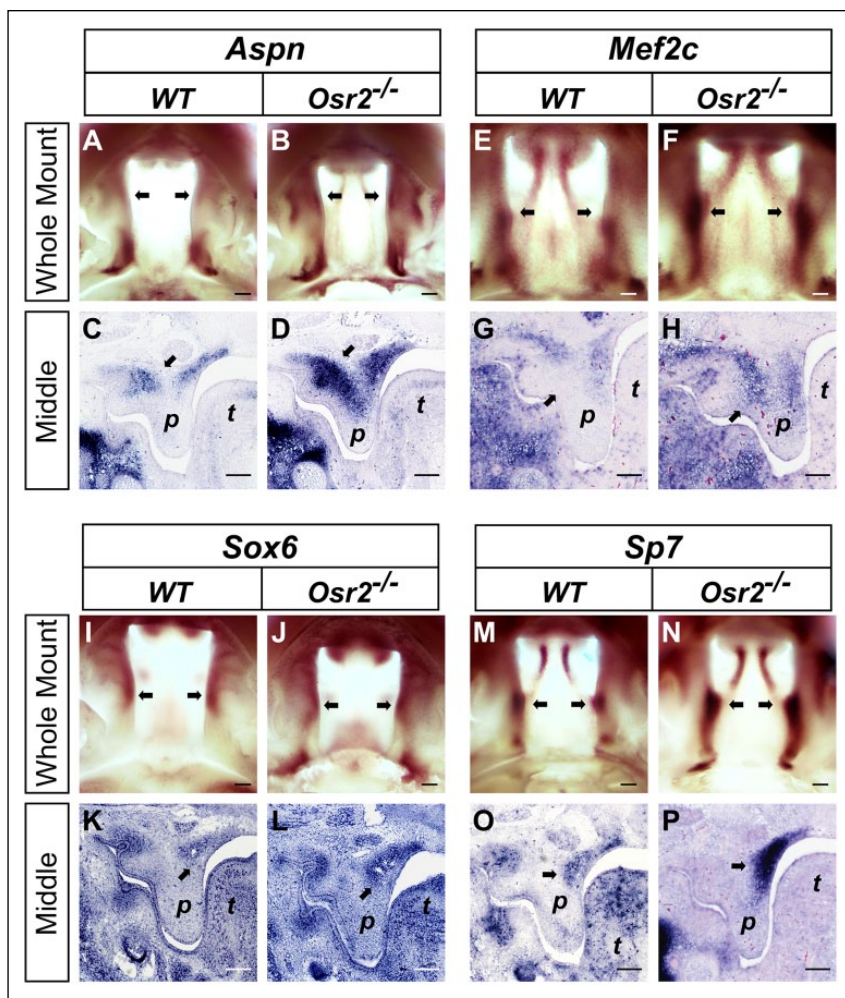


Figure 3. Comparison of patterns of expression of *Aspn*, *Mef2c*, *Sox6*, and *Sp7* mRNAs in embryonic day 13.5 *Osr2*^{-/-} mutant and wild-type embryos by whole mount and section in situ hybridization. Whole mount images show oral views of the palatal shelves, whereas the “middle” rows show coronal sections from the middle region of the palatal shelves. (A–D) Expression patterns of *Aspn* mRNAs. (E–H) Expression patterns of *Mef2c* mRNAs. (I–L) Expression patterns of *Sox6* mRNAs. (M–P) Expression patterns of *Sp7* mRNAs. Arrows point to regions of differential expression. p, palatal shelf; t, tongue. Scale bars, 100 μ m.

genes encoding members of class 3 semaphorins, *Sema3a*, *Sema3d*, and *Sema3e* (Ryynanen et al. 2017), were each significantly upregulated in the *Osr2*^{RFP/-} mutant palatal mesenchyme in comparison with that in the *Osr2*^{RFP/+} littermates. RT-qPCR analyses validated significant upregulation of expression of each of these genes in *Osr2*^{RFP/-} palatal mesenchyme (Fig. 1C). In situ hybridization analysis revealed that expression of *Sema3a* and *Sema3d* mRNAs were dramatically upregulated in the middle and posterior regions of palatal shelf mesenchyme in *Osr2*^{-/-} embryos in comparison with wild-type littermates at E13.5 (Fig. 4A–P). Whereas *Sema3e* mRNA expression was restricted to the medial side of anterior palatal mesenchyme in E13.5 wild-type embryos (Fig. 4Q, S, U, W), it was upregulated in the anterior and posterior, but not in the middle regions of palatal mesenchyme in *Osr2*^{-/-} embryos (Fig. 4R, T, V, X).

The class 3 semaphorins are secreted proteins and function through binding to receptor complexes consisting of neuropilins

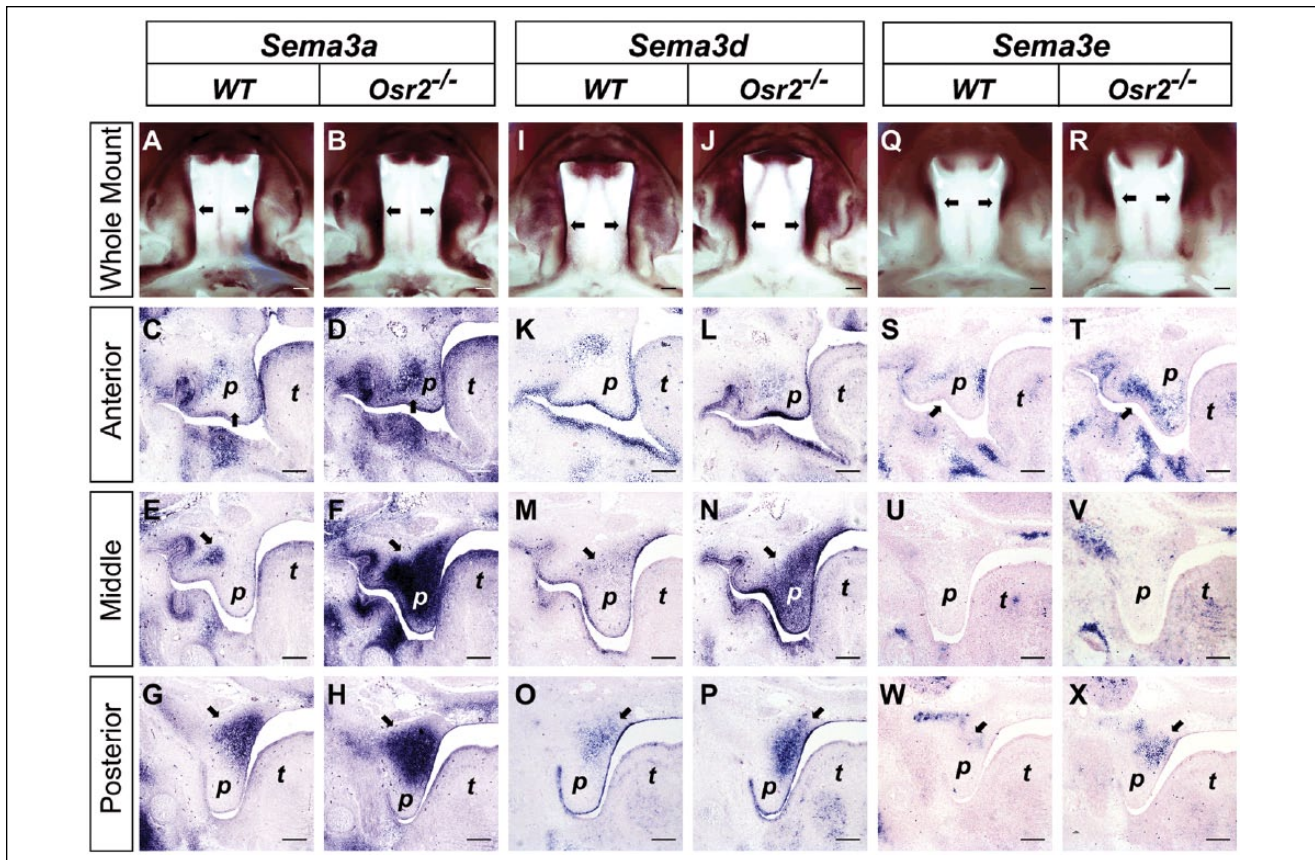


Figure 4. Comparison of patterns of expression of *Sema3a*, *Sema3d*, and *Sema3e* mRNAs in embryonic day 13.5 *Osr2*^{-/-} mutant and wild-type embryos. Whole mount images (top row) show oral views of the palatal shelves, whereas the “anterior,” “middle,” and “posterior” rows show coronal sections from regions of the palatal shelves. (A–H) Expression patterns of *Sema3a* mRNAs. (I–P) Expression patterns of *Sema3d* mRNAs. (Q–X) Expression patterns of *Sema3e* mRNAs. Arrows point to regions of differential expression. p, palatal shelf; t, tongue. Scale bar, 100 μ m.

and plexins (reviewed by Valdembrì et al. 2016). *Nrp1*, *Nrp2*, and *Plexin1* were expressed at relatively low levels throughout the palatal mesenchyme at E13.5 (Appendix Fig. 2). RNA-seq and RT-qPCR analyses showed that expression of *Nrp2* mRNAs was upregulated in *Osr2* mutant palatal mesenchyme at E13.5 in comparison with control embryos (Appendix Fig. 2, Appendix Table 1). In addition, *Sema3e* has been shown to bind to PlexinD1 to regulate vascular pattern in a neuropilin-independent manner (Gu et al. 2005). We found that *PlexinD1* mRNAs were highly expressed in endothelial cells in the palatal shelves in both control and *Osr2* mutant embryos (Appendix Fig. 2M–P). Thus, increased expression of the *Sema3* ligands in *Osr2* mutant palatal mesenchyme might affect palate development directly through signaling to palatal mesenchyme cells or indirectly through regulating the vasculature.

We next examined the promoter sequences of each of these *Sema3* genes and found that each contains several sites matching the previously determined *Osr2*-binding core sequence, GCTAC(T/C)GT (Kawai et al. 2007; Badis et al. 2009; Fig. 5A). To test if *Osr2* is able to repress the promoter activity of these genes, we constructed luciferase reporter vectors containing 3 kb of genomic sequence immediately upstream of the transcriptional start site of these genes and performed

cotransfection assays with an *Osr2* expression vector in NIH/3T3 cells. As shown in Figure 5B, luciferase reporter expression driven by the *Sema3a* and *Sema3d* promoters, respectively, was significantly suppressed by *Osr2* coexpression, whereas luciferase expression from the *Sema3e* promoter was not significantly affected.

To verify that *Osr2* directly regulates expression of the *Sema3a* and *Sema3d* genes in developing palatal mesenchyme in vivo, we took advantage of the *Osr2*^{Myc-Osr2AKi/+} mice, which carry the *Osr2A* cDNA knockin at the endogenous *Osr2* locus and contain an in-frame fusion of a 6xMYC epitope tag coding sequence immediately 5' to the translation start codon. *Osr2*^{Myc-Osr2AKi/-} mice exhibit normal palate development, indicating that the Myc-Osr2A protein expressed from the knockin allele is sufficient to replace endogenous *Osr2* function in palate development (Gao et al. 2009). We performed chromatin immunoprecipitation (ChIP) analysis of microdissected palatal shelf tissues from E13.5 *Osr2*^{Myc-Osr2AKi/Myc-Osr2AKi} embryos with a monoclonal antibody specific for the MYC epitope tag, followed by real-time PCR analysis of enrichment of DNA fragments containing the *Osr2*-binding core sequence in the promoter regions of the *Sema3a*, *Sema3d*, and *Sema3e* genes. As shown in Figure 5C, *Osr2* protein bound to 1 and 3 predicted sites in the 3-kb

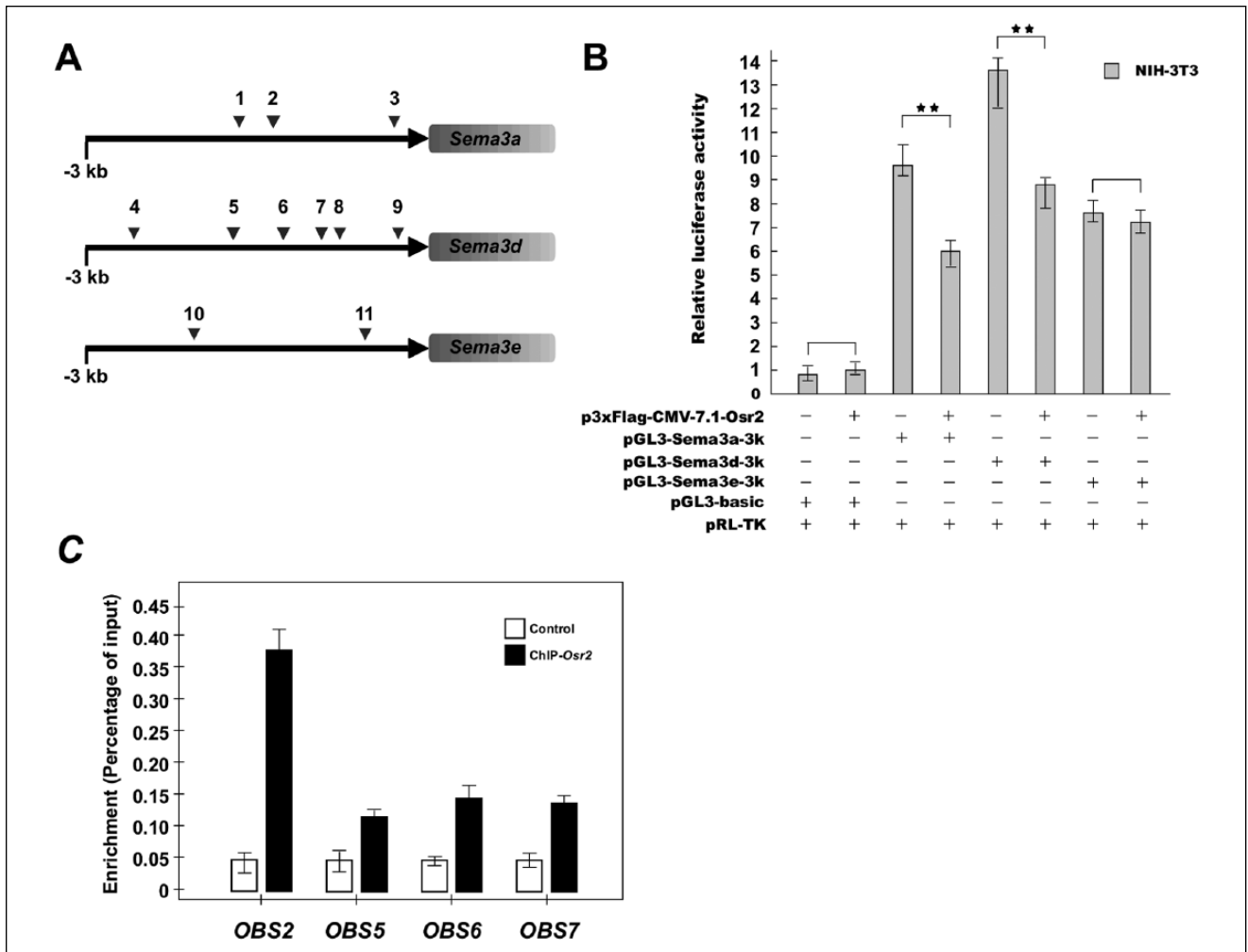


Figure 5. Osr2 binds to the promoter regions of *Sema3a* and *Sema3d* genes in the developing palatal mesenchyme and represses luciferase reporter gene expression driven by these promoters. **(A)** Diagram of putative Osr2-binding sites in the promoter regions of *Sema3a*, *Sema3d*, and *Sema3e*. **(B)** Coexpression of Osr2 repressed activity of *Sema3a* and *Sema3d*, but not *Sema3e*, promoters in cotransfected NIH/3T3 cells. **(C)** ChIP-qPCR analyses revealed enrichment of Osr2-binding to specific sites in the *Sema3a* and *Sema3d* promoter sequences. OBS, Osr2-binding site (2, 5, 6, 7 correspond to the putative sites marked in panel A). Error bars indicates standard error of the mean.

promoter region of the *Sema3a* and *Sema3d* genes, respectively, in the developing palatal mesenchyme. With the differential expression of *Sema3a* and *Sema3d* mRNAs in the palatal mesenchyme in *Osr2*^{-/-} and control embryos and the effects of Osr2 on expression of the promoter-luciferase constructs in transfected NIH/3T3 cells, these results indicate that Osr2 directly regulates expression of *Sema3a* and *Sema3d* in the developing palatal mesenchyme.

Discussion

Although previous studies have clearly demonstrated a crucial role for Osr2 in palatal shelf growth and morphogenesis, the molecular mechanism mediating Osr2 function in palate development is largely unknown. In this study, we used whole transcriptome expression profiling, RT-qPCR, and in situ hybridization analyses, in combination with ChIP-qPCR identification of endogenous Osr2 binding at promoter sequences in the

developing palatal shelves and promoter-luciferase reporter assays to uncover transcriptional target genes regulated by Osr2 in palate development. Gene ontology analysis of differentially expressed genes between *Osr2*^{RFP/-} and *Osr2*^{RFP/+} embryonic palatal mesenchyme showed that expression of many signaling molecules and transcription factors involved in osteoblast differentiation is significantly increased in the *Osr2* mutant palatal mesenchyme cells. A previous study showed that overexpression of only the Osr2 DNA-binding domain caused decreased proliferation and differentiation of calvarial osteoblasts in transgenic mice, which led to the hypothesis that Osr2 positively regulates osteoblastic cell proliferation (Kawai et al. 2007). The increase in expression of multiple positive regulators of osteogenesis in the *Osr2* mutant palatal mesenchyme, with our previous finding that *Osr2*^{-/-} embryos exhibit a significant reduction in palatal mesenchyme proliferation (Lan et al. 2004), suggests that enhanced osteogenic differentiation of the developing palatal mesenchyme contributes to cleft palate pathogenesis in *Osr2*-deficient mice.

Our RNA-seq and in situ hybridization assays reveal a crucial role for *Osr2* in preventing aberrant activation of expression of 3 closely related class 3 semaphorins. Semaphorins were initially isolated as negative regulators of axonal guidance in neural development (Kolodkin et al. 1993; Luo et al. 1993). Subsequent studies have shown that these signaling molecules regulate many developmental and pathologic processes outside the nervous system, including cardiovascular development, endothelial motility, bone and lung morphogenesis, neural crest cell migration, cancer angiogenesis, and metastasis (Kruger et al. 2005; Yu and Moens 2005; Roth et al. 2009; Neufeld et al. 2012; Epstein et al. 2015; Valdembrì et al. 2016). Whereas the cellular effects of the dramatically increased expression of *Sema3a*, *Sema3d*, and *Sema3e* in the *Osr2* mutant palatal mesenchyme remain to be determined, recent studies have demonstrated a crucial role for these molecules, particularly *Sema3a*, in osteoblast differentiation (Hayashi et al. 2012; Fukuda et al. 2013; Ryyanen et al. 2017). It is possible that the increased *Sema3* signaling contributes to cleft palate pathogenesis through enhancing osteogenic differentiation of the palatal mesenchyme in *Osr2* mutant embryos. In addition, the increased expression of *Sema3e* might affect palate morphogenesis secondarily by affecting vascular pattern in the palatal shelves. Further studies are necessary to elucidate the contribution of *Osr2*-mediated regulation of class 3 semaphorins in palatal shelf growth and morphogenesis.

Author Contributions

X. Fu, contributed to acquisition, analysis, and interpretation of data, drafted and critically revised the manuscript; J. Xu, H. Liu contributed to acquisition and analysis of data, critically revised the manuscript; P. Chaturvedi, contributed to analysis of data, critically revised the manuscript; R. Jiang contributed to conception, design, analysis, and interpretation of data, drafted and critically revised the manuscript; Y. Lan contributed to conception, design, acquisition, analysis, and interpretation of data, drafted and critically revised the manuscript; All authors gave final approval and agree to be accountable for all aspects of the work.

Acknowledgments

We thank Lynessa McGee for technical assistance and the Cincinnati Children's Hospital Medical Center Gene Expression and Sequencing Core Facilities for help with RNA-seq. This work was supported by National Institutes of Health / National Institute of Dental and Craniofacial Research grants DE013681 and DE018401. The authors declare no potential conflicts of interest with respect to the authorship and/or publication of this article.

References

- Almaidhan A, Cesario J, Landin Malt A, Zhao Y, Sharma N, Choi V, Jeong J. 2014. Neural crest-specific deletion of *Ldb1* leads to cleft secondary palate with impaired palatal shelf elevation. *BMC Dev Biol.* 14:3.
- Badis G, Berger MF, Philippakis AA, Talukder S, Gehrke AR, Jaeger SA, Chan ET, Metzler G, Vedenko A, Chen X, et al. 2009. Diversity and complexity in DNA recognition by transcription factors. *Science.* 324(5935):1720–1723.
- Brunskill EW, Potter SS. 2012. RNA-Seq defines novel genes, RNA processing patterns and enhancer maps for the early stages of nephrogenesis: Hox supergenes. *Dev Biol.* 368(1):4–17.
- Bush JO, Jiang R. 2012. Palatogenesis morphogenetic and molecular mechanisms of secondary palate development. *Development.* 139(2):231–243.
- Chen J, Aronow BJ, Jegga AG. 2009. Disease candidate gene identification and prioritization using protein interaction networks. *BMC Bioinformatics.* 10:73.
- Dixon MJ, Marazita ML, Beaty TH, Murray JC. 2011. Cleft lip and palate: understanding genetic and environmental influences. *Nat Rev Genet.* 12(3):167–178.
- Epstein JA, Aghajanian H, Singh MK. 2015. Semaphorin signaling in cardiovascular development. *Cell Metab.* 21(2):163–173.
- Fukuda T, Takeda S, Xu R, Ochi H, Sunamura S, Sato T, Shibata S, Yoshida Y, Gu Z, Kimura A, et al. 2013. *Sema3A* regulates bone-mass accrual through sensory innervations. *Nature.* 497(7450):490–493.
- Funato N, Nakamura M, Yanagisawa H. 2015. Molecular basis of cleft palates in mice. *World J Biol Chem.* 6(3):121–138.
- Gao Y, Lan Y, Ovitt CE, Jiang R. 2009. Functional equivalence of the zinc finger transcription factors *Osr1* and *Osr2* in mouse development. *Dev Biol.* 328(2):200–209.
- Gu C, Yoshida Y, Livet J, Reimert DV, Mann F, Merte J, Henderson CE, Jessel TM, Kolodkin AL, Ginty DD. 2005. Semaphorin 3E and plexin-D1 control vascular pattern independently of neuropilins. *Science.* 307(5707):265–268.
- Hayashi M, Nakashima T, Taniguchi M, Kodama T, Kumanogoh A, Takayanagi H. 2012. Osteoprotection by semaphorin 3A. *Nature.* 485(7396):69–74.
- Kawai S, Yamauchi M, Wakisaka S, Ooshima T, Amano A. 2007. Zinc-finger transcription factor odd-skipped related 2 is one of the regulators in osteoblast proliferation and bone formation. *J Bone Miner Res.* 22(9):1362–1372.
- Kolodkin A, Matthes D, Goodman C. 1993. The semaphorin genes encode a family of transmembrane and secreted growth cone guidance molecules. *Cell.* 75(7):1389–1399.
- Kruger R, Aurandt J, Guan K. 2005. Semaphorins command cells to move. *Nat Rev Mol Cell Biol.* 6(10):789–800.
- Lan Y, Jiang R. 2009. Sonic hedgehog signaling regulates reciprocal epithelial-mesenchymal interactions controlling palatal outgrowth. *Development.* 136(8):1387–1396.
- Lan Y, Kingsley P, Cho E, Jiang R. 2001. *Osr2*, a new mouse gene related to drosophila odd-skipped, exhibits dynamic expression patterns during craniofacial, limb, and kidney development. *Mech Dev.* 107(1–2):175–179.
- Lan Y, Ovitt CE, Cho ES, Maltby KM, Wang Q, Jiang R. 2004. Odd-skipped related 2 (*Osr2*) encodes a key intrinsic regulator of secondary palate growth and morphogenesis. *Development.* 131(13):3207–3216.
- Lan Y, Xu J, Jiang R. 2015. Cellular and molecular mechanisms of palatogenesis. *Curr Top Dev Biol.* 115:59–84.
- Lane J, Kaartinen V. 2014. Signaling networks in palate development. *Wiley Interdiscip Rev Syst Biol Med.* 6(3):271–278.
- Luo Y, Raible D, Raper J. 1993. Collapsin: a protein in brain that induces the collapse and paralysis of neuronal growth cones. *Cell.* 75(2):217–227.
- Neufeld G, Sabag AD, Rabinovitz N, Kessler O. 2012. Semaphorins in angiogenesis and tumor progression. *Cold Spring Harb Perspect Med.* 2(1):a006718.
- Peters H, Neubüser A, Kratochwil K, Balling R. 1998. Pax9-deficient mice lack pharyngeal pouch derivatives and teeth and exhibit craniofacial and limb abnormalities. *Genes Dev.* 12(17):2735–2747.
- Prescott N, Lees M, Winter R, Malcolm S. 2000. Identification of susceptibility loci for nonsyndromic cleft lip with or without cleft palate in a two stage genome scan of affected sib-pairs. *Hum Genet.* 106(3):345–350.
- Roth L, Koncina E, Satkauskas S, Crémel G, Aunis D, Bagnard D. 2009. The many faces of semaphorins: from development to pathology. *Cell Mol Life Sci.* 66(4):649–666.
- Ryyanen J, Kriebitzsch C, Meyer MB, Janssens I, Pike JW, Verlinden L, Verstuyf A. 2017. Class 3 semaphorins are transcriptionally regulated by 1,25(OH)₂D₃ in osteoblasts. *J Steroid Biochem Mol Biol.* 173:185–193.
- Valdembrì D, Regano D, Maione F, Giraudo E, Serini G. 2016. Class 3 semaphorins in cardiovascular development. *Cell Adh Migr.* 10(6):641–651.
- Xu J, Liu H, Lan Y, Aronow BJ, Kalinichenko VV, Jiang R. 2016. A Shh-Foxf-Fgf18-Shh molecular circuit regulating palate development. *PLoS Genet.* 12(1):e1005769.
- Yu HH, Moens CB. 2005. Semaphorin signaling guides cranial neural crest cell migration in zebrafish. *Dev Biol.* 280(2):373–385.
- Zhang Y, Zhao X, Hu Y, St Amand T, Zhang M, Ramamurthy R, Qiu M, Chen Y. 1999. *Msx1* is required for the induction of patched by sonic hedgehog in the mammalian tooth germ. *Dev Dyn.* 215(1):45–53.
- Zhou J, Gao Y, Lan Y, Jia S, Jiang R. 2013. Pax9 regulates a molecular network involving *Bmp4*, *Fgf10*, *Shh* signaling and the *Osr2* transcription factor to control palate morphogenesis. *Development.* 140(23):4709–4718.
- Zhou J, Gao Y, Zhang Z, Zhang Y, Maltby KM, Liu Z, Lan Y, Jiang R. 2011. *Osr2* acts downstream of Pax9 and interacts with both *Msx1* and Pax9 to pattern the tooth developmental field. *Dev Biol.* 353(2):344–353.